A Characterization of Asian Oral Cancer Spheroids using the Liquid Overlay Technique

Pema Yangzom[*1,2], Poramaporn Klanrit[1,2], Poramate Klanrit[3,4]

[1]Department of Oral Biomedical Sciences, Faculty of Dentistry, KhonKaen University, KhonKaen, Thailand
[2]Research Group of Chronic Inflammatory Oral Diseases and Systemic Diseases Associated with Oral Health, Faculty of Dentistry, KhonKaen University, KhonKaen, Thailand
[3]Department of Biochemistry, Faculty of Medicine, KhonKaen University, KhonKaen, Thailand
[4]Cholangiocarcinoma Research Institute, KhonKaen University, KhonKaen, Thailand
[*]Corresponding author, E-mail:yangzoma77@gmail.com

Abstract

Multicellular tumor spheroids (MCTS) demonstrate a physiologically relevant microenvironment, similar growth kinetics, and almost identical cell-cell and cell-extracellular matrix interaction as those *in vivo*. MCTS can be cultured in a laboratory with various techniques; one of them is the liquid overlay technique that has not been performed in Asian oral cancer cell lines; ORL-48 and ORL-136. This technique is inexpensive and straightforward, with ease of maintenance and easy access to spheroids. The cancer cells are inhibited from adherence to the culture plates' surface by the liquid overlay technique to enable 3-dimension (3D) spheroid formation. This study aimed to grow and characterize the 3D spheroids of ORL-48 and ORL-136 with the liquid overlay technique. 10,000 and 25,000 cells per well of ORL-48 and ORL-136 were grown for seven days in U-bottomed 96-well plates pre-coated with 1% agarose. The characterization of spheroids' morphology, including shape, size, growth, surface characteristics, and core structure, was evaluated. The spheroids of two cell lines demonstrated different sizes but similar shape and growth characteristics. The spheroids of both cell lines showed a greater diameter with a cell density of 25,000 cells/well compared with a cell density of 10,000 cells/well. Besides, ORL-136 spheroids showed relatively smaller diameters for both cell densities as compared with ORL-48 spheroids. The spheroids became more compact on day 7 as compared with day 1. The hematoxylin and eosin-stained sections of the spheroids demonstrated densely packed sheets of pleomorphic squamous epithelial cells at their cores and 2-3 layers of squamous epithelial cells at their periphery. In conclusion, ORL-48 and ORL-136 spheroids were successfully developed via the liquid overlay technique. This model can be further studied to utilize for *in vitro* anticancer drug screening and could provide a suitable platform for future research on novel anticancer drugs' cytotoxicity.

Keywords: *multicellular tumor spheroids, oral squamous cell carcinoma cell lines, 3D microenvironment, liquid overlay technique*

1. Introduction

Among all malignant tumors, head and neck cancer is ranked the sixth most common, with 65,000 new cases per year, causing 35,000 deaths (Polz-Gruszka et al., 2014). Oral cancer, an essential subtype of head and neck cancer, is the third most common cancer and the leading cause of death in South-Central Asia (Petersen, 2003). Around 96% of oral cancers are oral squamous cell carcinoma. Oral squamous cell carcinoma is common among the most devastating head and neck cancer subtypes, especially in South, South East, and South Central Asia (Torre et al., 2015; Wong et al., 2017).

Despite the improvement in the treatment modalities including surgery, radiation, and chemotherapy, there is no improvement in prognosis for over 60 years, with only 50% of patients surviving for five years (Lee et al., 2014). The inferior prognosis of oral squamous cell carcinoma is due to local invasion, lymph node metastasis, and chemotherapy resistance (Chen et al., 2013). Increasing evidence has suggested that tumor microenvironment and tumor cell heterogeneity play an essential role in the determination of therapeutic response, causing resistance to chemotherapy (Silva et al., 2012).

Cell cultures have been used as one of the platforms to study cell biology, mechanisms of diseases, drug action, and tissue engineering development. It has been used in cancer research including *in vitro* testing

of many anticancer drugs and studies on disease mechanisms. The selection of the most appropriate cell culture method is essential for the researchers to understand tumor physiology better and to optimize chemotherapy or radiotherapy, paving the way for novel treatment strategies (Kapałczyńska et al., 2018).

The conventional 2D cell culture is the most frequently used method to investigate tumor cells *in vitro*. Despite its advantages such as ease of use, availability, and low maintenance cost, a 2D culture can differ considerably in its morphology with limited cell to cell and cell to extracellular matrix interactions. Furthermore, cells growing in a 2D culture differ from those cultured in a more physiological three-dimensional (3D) environment and tumor *in vivo* (Kadletz et al., 2015). In cytotoxicity assays, 2D cells are exposed to uniform drug concentration in a homogenous environment where cell interactions with the extracellular matrix and cell-cell contacts are substantially reduced (Kochanek, Close, and Johnston, 2019; Shan et al., 2018). 2D cells fail to recapitulate the complex 3D architecture, cell-cell, cell-extracellular matrix interaction, microenvironment, drug diffusion kinetics, and drug response of solid tumors *in vivo* (Baker and Chen, 2012; Fang and Eglen, 2017; Hongisto et al., 2013).

The tumor cells *in vivo* grow in 3 dimensions, exhibiting spatial arrangement of different cell zones, in dynamic interaction with their extracellular environment. This arrangement, in turn, affects their proliferation, differentiation, morphology, viability, gene expression, and cellular response to chemotherapeutic and radiotherapy treatment (Breslin and O'Driscoll, 2013). Since, the microenvironment within the 3D cell culture is more physiologically relevant, which recapitulates the *in vivo* microenvironment, resulting in cell-cell and cell-extracellular matrix signaling, the most analogous to a tumor *in vivo* is potentially 3D cell culture (Ryan et al., 2016). Besides, it can be a link between the traditional 2D cell culture and animal models (Breslin and O'Driscoll, 2013).

Numerous techniques have been developed to grow different spherical cancer models. Four spherical cancer models have been reported, namely multicellular tumor spheroids (MCTS), tumorspheres, tissue-derived tumorspheres (TDTS), and organotypic multicellular spheroids (OMS) (Weiswald, Bellet and Dangles-Marie, 2015). MCTS, one of the spherical cancer models, are generated from single-cell suspension culture in conventional, fetal bovine serum (FBS) supplemented medium without an exogenous extracellular matrix (ECM) in a non-adherent condition. MCTS exhibits growth kinetics similar to those in *vivo*, demonstrating inner necrotic core surrounded by quiescent cells and outer proliferating cells of 3-5 cell layers resulting in differential drug permeability (Sutherland, 1988). MCTS resembles avascular tumor nodules, micrometastasis, or intervascular regions of solid tumors (Ekert et al., 2014; Kochanek, Close, and Johnston, 2019; Shan et al., 2018; Wang et al., 2014). For the generation of MCTS, three techniques are reported in the literature, namely suspension culture, gel embedding culture, and scaffold culture. For the suspension culture, it can be classified into 1) liquid overlay technique/static suspension culture, 2) hanging drop method, and 3) device-assisted culture (Weiswald, Bellet and Dangles-Marie, 2015). Liquid overlay technique (LOT) is one of the suspension culture methods in which cells are inhibited from the adherence to the culture plates' surface. U-bottomed well plates are coated with a thin layer of agarose, agar or poly-HEMA, to prevent cells' adherence. Pre-coating with agarose has been used to successfully grow spheroids of the SCC9 cell line (Chen et al., 2012), SCC25 cell line (Lee et al., 2014), and OSCC cell lines (Sievers et al., 2018). Due to pre-coating, a cell-cell interaction is greater than a cell-surface interaction, therefore, allowing the aggregation and compaction of cells to form spheroids within 1-3 days for most cancer cell lines. The formation of spheroids occurs in three stages, comprising the first stage in which the assembly of dispersed cells as loose aggregates is found, followed by the second stage in which the cells pause to tightly aggregate as there is an accumulation of E-cadherin. Finally, the third stage shows the strong hemophilic interaction between E-cadherins to form compact spheroids (Costa et al., 2018; Lin et al., 2006).

Compared with other techniques of 3D cell culture, the spheroids generated by MCTS techniques, particularly liquid overlay technique, is simple, inexpensive with ease of maintenance, low shear force, easy access to spheroids, a high success rate of initiation, better tumor growth, and suitable for high throughput drug screening (Costa et al., 2018; Weiswald, Bellet and Dangles-Marie, 2015). LOT is one of the most powerful techniques to generate spheroids reproducibly with a high yield rate (Metzger et al., 2011).

In literature, there have been reports on the characterization of 3D spheroids/MCTS in HNSCC (head and neck squamous cell carcinoma) cell lines (CAL33, CAL27, FaDu, Um-22B, Um-SCC-1, SCC9, Detroit-562, BICR56, OSC-19, PCI-52, and PCI-13), human tongue cancer cell line (SAS), human gingival SCC cell line (OECM) (Chen et al., 2012; Kochanek, Close and Johnston, 2019) and two reports on the characterization of spheroids in an ORL-48 cell line (Furqan et al., 2019; Wong et al., 2017). Wong et al. (2017) used the flicking technique, whereas Furqan et al. (2019) used the gel embedding technique to generate the ORL-48 cell lines' spheroids.

Malaysia's research group established ORL-48 and ORL-136 cell lines as Asian oral cancer cell lines in 2006. Both cell lines are human oral squamous cell carcinoma cell lines derived from surgically resected human gingiva and tongue specimens, respectively (Hamid et al., 2007).

There is no report on the characterization of spheroids derived from ORL-48 and ORL-136 cell lines using the liquid overlay technique to the best of our knowledge. Therefore, this study aimed to grow and characterize the 3D spheroids of ORL-48 and ORL-136 generated by the liquid overlay technique. The spheroids were characterized with respect to their shape, size, growth, surface, and core characteristics.

2. Objectives

1) To create spheroids of ORL-48 and ORL-136 using the liquid overlay technique
2) To determine the characteristics of ORL-48 and ORL-136 spheroids
3) To compare the differences in morphology of oral cancer spheroids, including shape, size, surface, and growth among spheroids of the same cell line growing in different days and between two oral cancer spheroids for each day of cell culture

3. Materials and methods

3.1 Study design: The study was experimental laboratory research, in which the characterization of the ORL-48 and ORL-136 cancer cell lines' spheroids was carried out.

3.2 Cell lines used in the study: Two oral squamous cell carcinoma cell lines, namely ORL-48 and ORL-136 cell lines, were used for the characterization of Asian oral cancer cell lines' spheroids. Both cell lines were kindly provided by Prof. Cheong Sok Ching of the Head and Neck Cancer Research Team, Cancer Research Malaysia, Malaysia.

3.3 2D cell culture: ORL-48 and ORL-136 cells were cultured in DMEM/F12medium (Gibco™, NY, USA) supplemented with 10% fetal bovine serum (Gibco™, NY, USA), 0.4 µg/ml of hydrocortisone (Sigma-Aldrich, MO, USA), and 1% antibiotic-antimycotic (Gibco™, NY, USA). Cells were grown in a T25 flask (Corning®, VA, USA) and incubated in a humidified atmosphere of 5% CO_2 at 37°C.

3.4 Trypsinization and cell counting: The old medium was removed followed by a PBS (phosphate-buffered saline, Gibco™, NY, USA) wash. The monolayer was trypsinized with 0.25% Trypsin (Gibco™, NY, USA) and incubated in a humidified atmosphere of 5% CO_2 at 37°C for 5 minutes. The cell numbers were calculated using a hemocytometer. The cell densities used were 1×10^4 cells/well and 2.5×10^4 cells/well for each of the cell lines of ORL-48 and ORL-136.

3.5 Pre-coating the U-bottomed 96-well plates with agarose: 1% agarose solution (Vivantis, Selangor Darul Ehsan, Malaysia) was prepared in PBS and sterilized (Metzger et al., 2011). Subsequently, each well of the U-bottomed 96-well plates (Corning®, VA, USA) was coated by a thin layer of agarose. After coating, the well plates were left to dry for 30 minutes to 1 hour under the cell culture hood.

3.6 Generation of 3D spheroids: Seeding of 1×10^4 cells/well and 2.5×10^4 cells/well in 200 µl of DMEM/F12 complete medium per well were carried out in U-bottomed 96-well plates. The well plates were then

centrifuged at room temperature at 1,000 rpm for 10 minutes. Then, they were incubated in a humidified atmosphere of 5% CO_2 at 37ºC for seven days. The medium change was performed after three days.

3.7 Re-plating of spheroids: After seven days, the spheroids in the U-bottomed 96-well plate were transferred to a flat-bottomed 96-well plate (Corning®, VA, USA) using wide-bore pipette tips (Axygen, CA, USA). This re-plating procedure was carried out to demonstrate that the spheroids formed were a true spheroid. After re-plating, if the spheroids were disaggregated into a monolayer, it indicated that it was only an aggregation of cells. The morphology of spheroids in flat-bottomed wells was subsequently observed under the inverted phase-contrast microscope (ZEISSAXIO, Deutschland, Germany).

3.8 Hematoxylin and eosin staining of spheroids: After seven days, the spheroids were fixed overnight with 4% paraformaldehyde after a PBS wash in the U-bottomed 96-well plate. Then, the fixed spheroids were transferred from the U-bottomed 96-well plates to 1.5 ml microcentrifuge tubes. Paraformaldehyde was removed, followed by a PBS wash. After PBS wash, the spheroids were suspended in 100 µl of 0.35% agarose gel in the 6-well plates. Then, for embedding and cutting steps, the spheroids were dehydrated by an ethanol gradient from 70% to 100%. The spheroids were further dehydrated by 100% ethanol, followed by verification with xylene and impregnation with paraffin wax. Then, the spheroids were embedded in paraffin blocks and cut by MICROM HM 34OE (Thermo Scientific, Walldorf, Germany) microtome into 6 µm paraffin ribbons. For the staining process, the sections were deparaffinized, and hydrated followed by staining with Mayer's hematoxylin for 15 minutes. After being differentiated with acid alcohol (1 dip) and ammonia water (1 minute), it was counterstained with eosin for 5 seconds. Finally, the sections went through a series of dehydration and clearing (5 minutes each) followed by mounting. Then, the spheroids were observed under the optical microscope (ECLIPSE E200, Nikon, Tokyo, Japan).

3.9 Analysis of the morphology of spheroids/MCTS: The daily images of the MCTS were captured using the inverted phase-contrast microscope and image-ProPlus7 software with 5× and 10× magnification. The same software was used to measure the diameters (in micrometers) of the spheroids.

3.10 Statistics: The characteristics of the spheroids were presented by descriptive statistics. The sizes of spheroids were shown as the mean and SD, calculated by SPSS version 19 software.

4. Results and Discussion

4.1 Morphology of spheroids/MCTS

The cell lines, ORL-48 and ORL-136, formed spheroid/MCTS within 24 hours as observed under the inverted phase-contrast microscope (Figure 1). Most of both cell lines' spheroids were round in shape with an even periphery (Figure 1). Among ORL-48 and ORL-136 spheroids successfully formed, some had irregular shapes with an uneven periphery. There were some differences between ORL-48 and ORL-136 spheroids, and it was noticed that almost 100% of ORL-48 spheroids formed single rounded spheroids. However, for ORL-136 spheroids, it was 81% that formed single rounded spheroids. Also, ORL-136 spheroids appeared to create multiple small spheroids first and fused to form larger spheroids in due course of time. The spheroids of both cell lines showed inner darker core surrounded by outer lighter periphery like previously reported spheroids of HNSCC (Cal33, FaDu, Cal27, and PCI-13 cell lines) cell lines (Kochanek, Close and Johnston, 2019). The outer layer was mostly two to three layers of cell thickness, as observed on the seventh day. The inner core became more condensed on the second day but remained almost the same over seven days. Comparing the inner core on the first day and the seventh day, the spheroid on the seventh day showed a darker center. This appearance could indicate that the spheroids were becoming compacted faster on the second day. Then the compaction of spheroids became slower after the second day till the seventh day. In contrast, in previously reported HNSCC cell lines (Kochanek, Close, and Johnston, 2019), the spheroids became progressively darker with due course of time. ORL-48 and ORL-136 cell lines were resected from different anatomical sites, from the gingiva (stage IV, $T_4N_{2a}M_x$) and tongue (stage I, $T_1N_0M_0$), respectively. The expression of MDM2 protein and epidermal growth factor receptor (EGFR) are different in both cell lines. Besides, there are slight differences in gene mutations, hypermethylation, and gene deletion of tumor suppressor genes among the two cell lines (Hamid et al., 2007). The complexity and heterogeneity

of cancer cell lines are likely to have contributed to various spheroid formation sizes and spheroid formation success rates.

4.2 Size and growth of the spheroids

The size of the spheroids depended on the cell density per well. As expected, the spheroids with a cell density of 1×10^4 cells/well were relatively smaller than those spheroids with a cell density of 2.5×10^4 cells/well for both cell lines (Figure 1 and Figure 2). The mean diameters of the ORL-48 spheroids with a cell density of 1×10^4 cells/well from Day 1 to Day 7 were 245.61±14.62, 234.18±16.01, 227.81±13.57, 220.40±9.62, 211.69±12.74, 203.34±13.10, and 199.22±10.98 µm, respectively, and for a cell density of 2.5×10^4 cells/well, they were 334.94±22.58, 305.57±18.75, 295.92±19.54, 282.96±14.95, 272.02±17.81, 261.07±17.64, and 252.42±19.44 µm, respectively. Similar measurements for diameters of ORL-48 spheroids generated with different techniques and cell densities were reported (Wong et al., 2017). The MCTS of other HNSCC cell lines' spheroids demonstrated similar measurements for their diameters (Kochanek, Close, and Johnston, 2019; Sievers et al., 2018). The mean diameters of the ORL-136 spheroids with a cell density of 1×10^4 cells/well from Day 1 to Day 7 were 189.07±4.29, 180.14±6.13, 178.56±6.65, 181.00±5.04, 172.80±8.45, 166.18±10.54, and 159.84±8.90 µm, respectively and for a cell density of 2.5×10^4 cells/well, they were 272.02±8.35, 251.42±9.65, 247.10±8.72, 246.53±9.35, 238.46±11.88, 231.55±13.61, and 222.91±11.79 µm, respectively.

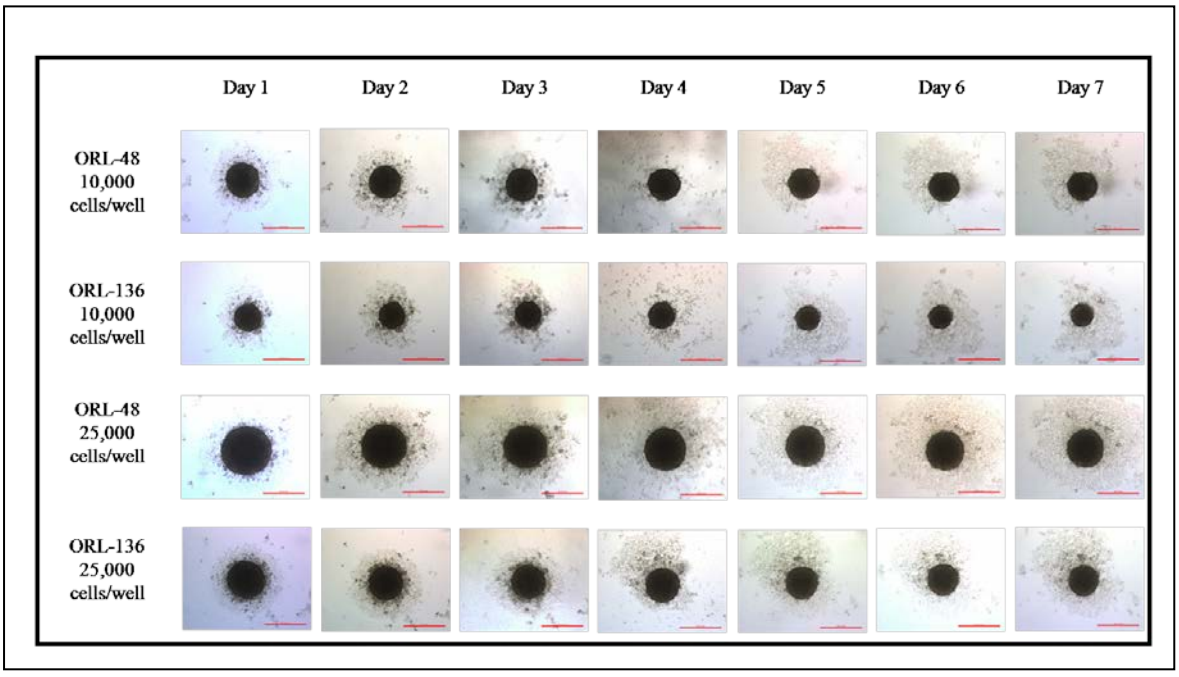

Figure 1 Growth of ORL-48 and ORL-136 MCTS /spheroids from day 1 to day 7 (representative images taken from the same well for each cell density and each cell line in U-bottomed 96-well plates) (Scale bar:300 µm)

Figure 1 shows the spheroids of ORL-48 and ORL-136 cell lines cultured in DMEM/F12 complete medium from day 1 to day 7 in agarose (1%) coated U-bottomed 96-well plates. The spheroids of both cell lines showed a greater diameter with a cell density of 2.5×10^4 cells/well compared with a cell density of 1×10^4cells/well. However, ORL-136 spheroids showed relatively smaller diameters for both cell densities as compared with ORL-48 spheroids. The spheroids became more compact on day 7 as compared with day 1. The size of the spheroids in both cell lines did not increase with time but showed a slight decline in sizes from day 1 to day 7.

The growth of the spheroids of different HNSCC cell lines showed varying growth patterns (Kochanek, Close, and Johnston, 2019). It varied depending on the cell lines, where some cell lines showed progressively increasing sizes while others showed diminishing sizes over time. However, some remained dormant, without showing any increase or decrease in sizes. Nonetheless, in the present study, there was a slight diminishing growth of spheroids, which could be due to the spheroids becoming tightly aggregated and compacted from loose aggregates over time.

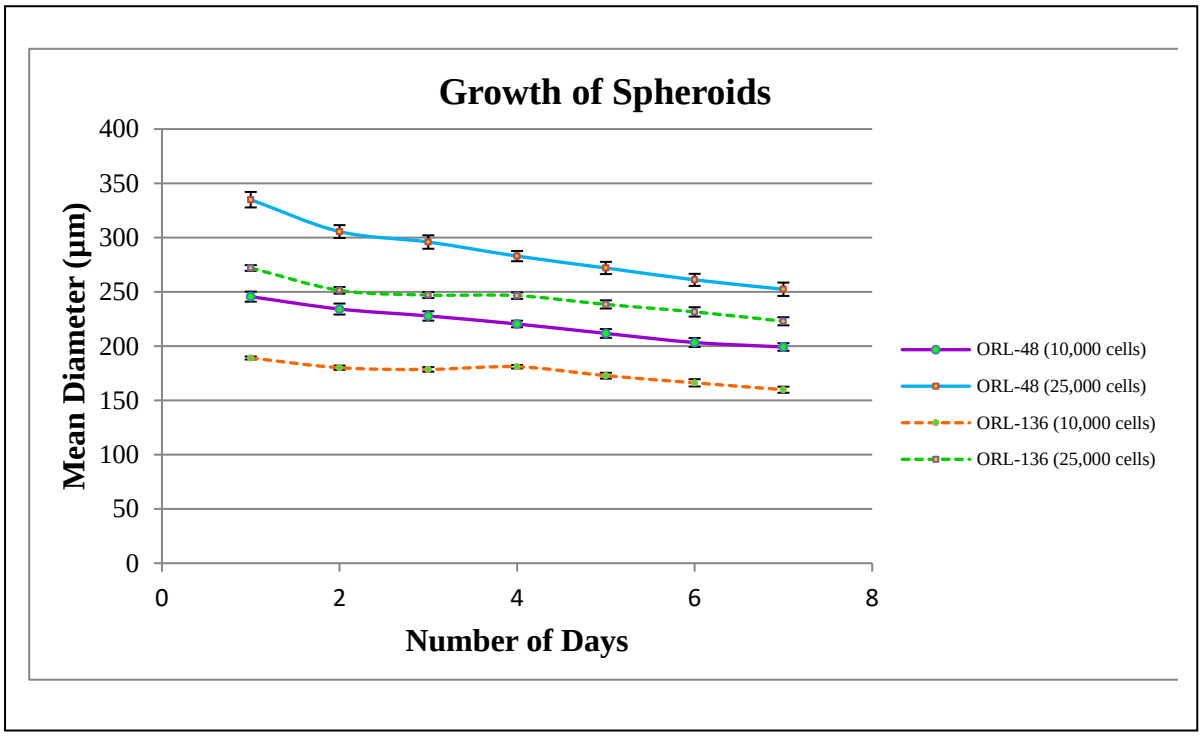

Figure 2 Changes in the mean diameters of the ORL-48 and ORL-136 cell lines' spheroids/MCTS for both cell densities (1×10^4 cells/well and 2.5×10^4 cells/well) from day 1 till day 7

Figure 2 shows the daily mean diameter of the spheroids of ORL-48 and ORL-136 cell lines grown every day from day 1 to day 7. The ORL-48 spheroids showed greater declining growth as compared with the spheroids of ORL-136 cell lines. The ORL-136 spheroids showed almost a dormant growth, particularly with a cell density of 1×10^4 cells/well.

4.3 The core structure of spheroids

The hematoxylin and eosin-stained sections of the spheroids of ORL-48 and ORL-136 cell lines at the seventh day showed the histological appearance of their core structures (Figure 3). The spheroids showed two distinct regions, the inner densely packed sheets of dysplastic squamous epithelial cells and the outer 2-3 layers of well-differentiated dysplastic squamous epithelial cells. The outer cell layers have maintained an epithelial architecture, while the inner core showed more pleomorphic cells. The inner core demonstrated apoptotic cells and keratin formation. The inner core occupied most of the spheroid structure as compared with few layers of outer cells. Ma et al. (2012) stated that the compact spheroid demonstrated three states of cells, the innermost necrotic cells, surrounded by quiescent cells, and outermost proliferative cells. Similarly, in the present study, the proliferative cells on the outermost cells demonstrated intact cell membrane with nuclear hyperchromatism. Besides, the inner core showed apoptotic cells, while quiescent cells showed

cellular and nuclear pleomorphism. The compacted sheets of dysplastic squamous epithelium in the inner core could explain the spheroids' inner darker core as observed under the inverted phase-contrast microscope. The thin 2-3 layers of squamous epithelial cells at the periphery could be the reason for the narrow outer, lighter region as observed under the inverted phase-contrast microscope.

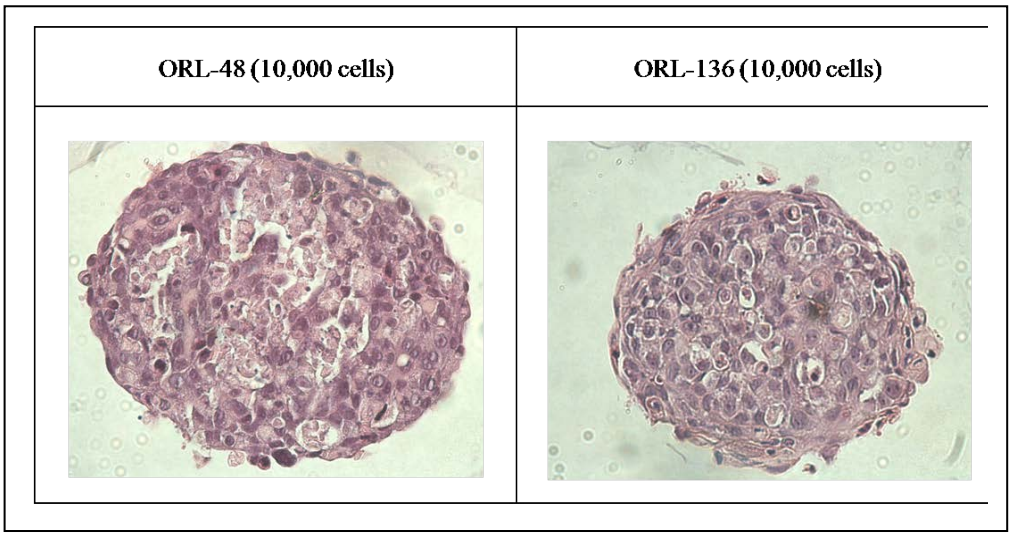

Figure 3 Hematoxylin and eosin-stained spheroids at day 7 for cell density of 10,000 cells/well for each cell line (400× magnification)

4.4 Spheroid re-plating

The re-plating of spheroids was carried out on day 7 to demonstrate that the spheroid is not merely an aggregation of cells. The spheroid will disaggregate into a monolayer in a flat-bottomed plate if it is just an aggregation of cells. If it remained intact as a spheroid, it indicates a true spheroid. Similar re-plating was also carried out in spheroids of ORL-48 cell lines cultured with a flicking technique (Wong et al., 2017). This result indicated that the spheroids formed in our laboratory setting were not merely an aggregation of cells but a compact spheroid (Figure 4).

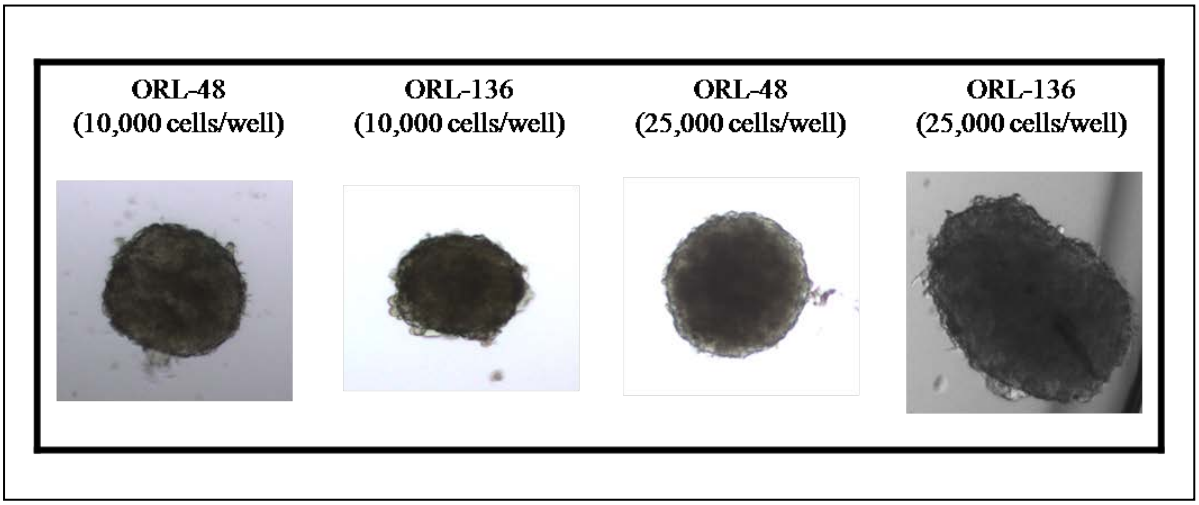

Figure 4 Re-plated spheroids of ORL-48 and ORL-136 cell lines in flat-bottomed 96-well plates at day 7

Figure 4 shows the spheroids of ORL-48 and ORL-136 cell lines after re-plating in flat-bottomed 96-well plates. The spheroids of both the cell lines for both cell densities were transferred from U-bottomed 96-well plates to flat-bottomed 96-well plates. The spheroids remained intact after re-plating on flat-bottomed 96-well plates.

5. Conclusion

The researchers have successfully generated the multicellular tumor spheroids of ORL-48 and ORL-136 cell lines using a liquid overlay technique. The characterization of their morphology, including shape, size, surface, growth characteristics, and inner core structure, was carried out by allowing the spheroids to grow for seven days. The sizes and success rate of spheroid formation were different among the cell lines. The spheroids of ORL-48 cell lines demonstrated larger diameters and a higher success rate of spheroid formation. The hematoxylin and eosin-stained sections of the spheroids demonstrated their core structures' histological appearance, which showed densely packed sheets of pleomorphic squamous epithelial cells at their cores and 2-3 layers of squamous epithelial cells at their periphery. This appearance explained the darker inner core and the lighter outer edge. These preliminary results suggest that this multicellular tumor model can be used as a 3D culture to screen novel anticancer drugs and study oral cancer pathogenesis. Further studies are required to improve and thoroughly examine the characteristics of oral cancer spheroids to apply for the development of patient-derived oral cancer spheroids in the future.

6. Acknowledgments

This work is supported by the Research Group of Chronic Inflammatory Oral Diseases and Systemic Diseases Associated with Oral Health, Faculty of Dentistry, KhonKaen University. Dr. Pema Yangzom is supported by scholarships from the Thailand International Cooperation Agency (TICA) and the Ministry of Health, Royal Government of Bhutan. The authors are grateful to Mr. Piboon Ngaonee, Mrs. Waraporn Phanphrom, Miss Pimpawadee Phukhum, Miss Pawinee Wisetsak, and Mrs. Supaporn Singhara for their generous help in making this research a success.

7. References

Baker, B. M., & Chen, C. S. (2012). Deconstructing the third dimension: how 3D culture microenvironments alter cellular cues. *Journal of cell science, 125*(Pt 13), 3015-3024. doi: 10.1242/jcs.079509

Breslin, S., & O'Driscoll, L. (2013). Three-dimensional cell culture: the missing link in drug discovery. *Drug Discov Today, 18*(5-6), 240-249. doi: 10.1016/j.drudis.2012.10.003

Chen, S.-F., Chang, Y.-C., Nieh, S., Liu, C.-L., Yang, C.-Y., & Lin, Y.-S. (2012). Nonadhesive Culture System as a Model of Rapid Sphere Formation with Cancer Stem Cell Properties. *PLoS One, 7*(2), e31864. doi: 10.1371/journal.pone.0031864

Chen, S.-F., Nieh, S., Jao, S.-W., Liu, C.-L., Wu, C.-H., Chang, Y.-C., . . . Lin, Y.-S. (2012). Quercetin suppresses drug-resistant spheres via the p38 MAPK-Hsp27 apoptotic pathway in oral cancer cells. *PLoS One, 7*(11), e49275-e49275. doi: 10.1371/journal.pone.0049275

Chen, S. F., Nien, S., Wu, C. H., Liu, C. L., Chang, Y. C., & Lin, Y. S. (2013). Reappraisal of the anticancer efficacy of quercetin in oral cancer cells. *J Chin Med Assoc, 76*(3), 146-152. doi: 10.1016/j.jcma.2012.11.008

Costa, E. C., de Melo-Diogo, D., Moreira, A. F., Carvalho, M. P., & Correia, I. J. (2018). Spheroids Formation on Non-Adhesive Surfaces by Liquid Overlay Technique: Considerations and Practical Approaches. *13*(1). doi: 10.1002/biot.201700417

Ekert, J. E., Johnson, K., Strake, B., Pardinas, J., Jarantow, S., Perkinson, R., & Colter, D. C. (2014). Three-dimensional lung tumor microenvironment modulates therapeutic compound responsiveness in vitro--implication for drug development. *PLoS One, 9*(3), e92248-e92248. doi: 10.1371/journal.pone.0092248

Fang, Y., & Eglen, R. M. (2017). Three-Dimensional Cell Cultures in Drug Discovery and Development. *SLAS discovery : advancing life sciences R & D, 22*(5), 456-472. doi: 10.1177/1087057117696795

Furqan, M., Huma, Z., Ashfaq, Z., Nasir, A., Ullah, R., Bilal, A., . . . Hussain, I. (2019). Identification and evaluation of novel drug combinations of Aurora kinase inhibitor CCT137690 for enhanced efficacy in oral cancer cells. *18*(18), 2281-2292. doi: 10.1080/15384101.2019.1643658

Hamid, S., Lim, K. P., Zain, R. B., Ismail, S. M., Lau, S. H., Mustafa, W. M., . . . Cheong, S. C. (2007). Establishment and characterization of Asian oral cancer cell lines as in vitro models to study a disease prevalent in Asia. *Int J Mol Med, 19*(3), 453-460.

Hongisto, V., Jernström, S., Fey, V., Mpindi, J. P., Kleivi Sahlberg, K., Kallioniemi, O., & Perälä, M. (2013). High-throughput 3D screening reveals differences in drug sensitivities between culture models of JIMT1 breast cancer cells. *PLoS One, 8*(10), e77232. doi: 10.1371/journal.pone.0077232

Kadletz, L., Heiduschka, G., Domayer, J., Schmid, R., Enzenhofer, E., & Thurnher, D. (2015). Evaluation of spheroid head and neck squamous cell carcinoma cell models in comparison to monolayer cultures. *Oncol Lett, 10*(3), 1281-1286. doi: 10.3892/ol.2015.3487

Kapałczyńska, M., Kolenda, T., Przybyła, W., Zajączkowska, M., Teresiak, A., Filas, V., . . . Lamperska, K. (2018). 2D and 3D cell cultures - a comparison of different types of cancer cell cultures. *Archives of medical science : AMS, 14*(4), 910-919. doi: 10.5114/aoms.2016.63743

Kochanek, S. J., Close, D. A., & Johnston, P. A. (2019). High Content Screening Characterization of Head and Neck Squamous Cell Carcinoma Multicellular Tumor Spheroid Cultures Generated in 384-Well Ultra-Low Attachment Plates to Screen for Better Cancer Drug Leads. *Assay Drug Dev Technol, 17*(1), 17-36. doi: 10.1089/adt.2018.896

Lee, C., Lee, C., Atakilit, A., Siu, A., & Ramos, D. M. (2014). Differential spheroid formation by oral cancer cells. *Anticancer Res, 34*(12), 6945-6949.

Lin, R. Z., Chou, L. F., Chien, C. C., & Chang, H. Y. (2006). Dynamic analysis of hepatoma spheroid formation: roles of E-cadherin and beta1-integrin. *Cell Tissue Res, 324*(3), 411-422. doi: 10.1007/s00441-005-0148-2

Ma, H. L., Jiang, Q., Han, S., Wu, Y., Cui Tomshine, J., Wang, D., . . . Liang, X. J. (2012). Multicellular tumor spheroids as an in vivo-like tumor model for three-dimensional imaging of chemotherapeutic and nano material cellular penetration. *Mol Imaging, 11*(6), 487-498.

Metzger, W., Sossong, D., Bächle, A., Pütz, N., Wennemuth, G., Pohlemann, T., & Oberringer, M. (2011). The liquid overlay technique is the key to formation of co-culture spheroids consisting of primary osteoblasts, fibroblasts and endothelial cells. *Cytotherapy, 13*(8), 1000-1012. doi: 10.3109/14653249.2011.583233

Petersen, P. E. (2003). The World Oral Health Report 2003: continuous improvement of oral health in the 21st century--the approach of the WHO Global Oral Health Programme. *Community Dent Oral Epidemiol, 31 Suppl 1*, 3-23. doi: 10.1046/j..2003.com122.x

Polz-Gruszka, D., Macieląg, P., Fołtyn, S., & Polz-Dacewicz, M. (2014). Oral squamous cell carcinoma (OSCC) – molecular, viral and bacterial concepts. *Journal of Pre-Clinical and Clinical Research, 8*(2), 61-66. doi: 10.26444/jpccr/71469

Ryan, S. L., Baird, A. M., Vaz, G., Urquhart, A. J., Senge, M., Richard, D. J., . . . Davies, A. M. (2016). Drug Discovery Approaches Utilizing Three-Dimensional Cell Culture. *Assay Drug Dev Technol, 14*(1), 19-28. doi: 10.1089/adt.2015.670

Shan, F., Close, D. A., Camarco, D. P., & Johnston, P. A. (2018). High-Content Screening Comparison of Cancer Drug Accumulation and Distribution in Two-Dimensional and Three-Dimensional Culture Models of Head and Neck Cancer. *Assay Drug Dev Technol, 16*(1), 27-50. doi: 10.1089/adt.2017.812

Sievers, D., Bunzendahl, J., Frosch, A., Perske, C., Hemmerlein, B., Schliephake, H., & Brockmeyer, P. (2018). Generation of highly differentiated BHY oral squamous cell carcinoma multicellular spheroids. *Mol Clin Oncol, 8*(2), 323-325. doi: 10.3892/mco.2017.1514

Silva, S., Heir, M., Mlynarek, A., Kowalski, L., & Alaoui -Jamali, M. A. (2012). Recurrent Oral Cancer: Current and Emerging Therapeutic Approaches. *Frontiers in Pharmacology, 3*(149). doi: 10.3389/fphar.2012.00149

Sutherland, R. M. (1988). Cell and environment interactions in tumor microregions: the multicell spheroid model. *Science, 240*(4849), 177-184. doi: 10.1126/science.2451290

Torre, L. A., Bray, F., Siegel, R. L., Ferlay, J., Lortet-Tieulent, J., & Jemal, A. (2015). Global cancer statistics, 2012. *CA Cancer J Clin, 65*(2), 87-108. doi: 10.3322/caac.21262

Wang, C., Tang, Z., Zhao, Y., Yao, R., Li, L., & Sun, W. (2014). Three-dimensional in vitro cancer models: a short review. *Biofabrication, 6*(2), 022001. doi: 10.1088/1758-5082/6/2/022001

Weiswald, L. B., Bellet, D., & Dangles-Marie, V. (2015). Spherical cancer models in tumor biology. *Neoplasia, 17*(1), 1-15. doi: 10.1016/j.neo.2014.12.004

Wong, S., Soon, C., Tee, K., Leong, w. y., Ahmad, M., & Cheong, S. (2017). 3D Oral Squamous Cell Carcinoma Microtissues Grown in Calcium Alginate Microbeads. *Annual Research & Review in Biology, 13*, 1-12. doi: 10.9734/ARRB/2017/33526